

## Scaling of granular temperature in a vibrated granular bed

V. Zivkovic,<sup>1,\*</sup> M. J. Biggs,<sup>1</sup> and D. H. Glass<sup>2</sup>

<sup>1</sup>*School of Chemical Engineering, The University of Adelaide, Adelaide, SA, 5005, Australia*

<sup>2</sup>*Institute for Materials and Processes, The University of Edinburgh, Sanderson Building, King's Buildings, Mayfield Road, Edinburgh EH9 3JL, United Kingdom*

(Received 11 July 2010; revised manuscript received 10 January 2011; published 28 March 2011)

Granular temperature underpins the kinetic theory of granular flows as well as models for heat transfer, segregation, erosion, attrition, and aggregation in various granular systems. It is generally thought that granular temperature in vibrated granular systems scales with the square of the peak vibrational velocity. However, careful diffusing wave spectroscopy experiments and statistical analysis of data obtained from these for a three-dimensional vibrated bed of monodisperse glass particles reveals that the granular temperature is also significantly correlated with other vibrational parameters. Reexamination of previously published data obtained by others using alternative methods further supports our thus far unremarked upon observation reported here.

DOI: [10.1103/PhysRevE.83.031308](https://doi.org/10.1103/PhysRevE.83.031308)

PACS number(s): 45.70.-n, 05.20.Dd, 83.10.Pp, 42.62.Fi

### I. INTRODUCTION

Granular flow requires continuous energy supply, such as vibration, shearing, or interstitial fluid flow, because of the dissipative particle collisions which are dominant in the granular flow. Such energy input results in a random motion of particles which is quantified by the so-called granular temperature, which is proportional to the mean-square value of velocity fluctuations around the mean flow velocity,  $\langle \delta v^2 \rangle$ , a term first used by Ogawa [1]. The granular temperature is a key property in continuum models of granular flow [2,3], and it also underpins models for heat transfer [4], segregation [5], erosion [6], attrition [7], and aggregation [8] in various particle processing technologies.

Vibration of granular media occurs widely across technology (e.g., sorting of minerals) and nature (e.g., earthquakes). Many studies of such systems have focused on the scaling of the granular temperature with particular emphasis on the vibrational peak velocity. Kinetic theory considerations of a vibrated bed suggest a granular temperature scaling with the square of the peak velocity [9,10]. Experimental studies in highly fluidized two-dimensional (2D) [11,12] and dilute three-dimensional (3D) vibrated granular system [13–15] support this theoretical prediction. On the other hand, some experimental studies suggest a power-law relation with an exponent  $\sim 1.5$  [9,16,17], similar to numerical simulation results [18]. Two more recent experimental studies of the granular temperature scaling in highly dense 3D vibrated granular beds [19,20] were also, however, in line with the granular kinetic theory-based prediction [9,10].

Recent very careful experiments by us using the highly sensitive method of diffusing wave spectroscopy (DWS) have lead us to observe that granular temperature is not entirely independent of other vibrational parameters as commonly asserted. This finding is reported here. We first outline the experimental details, including an overview of DWS and details pertaining to the apparatus and the particulate materials used, and the experimental procedure. This is followed by a presentation of the results obtained using DWS to demonstrate

that a significant correlation exists between granular temperature and vibrational parameters beyond just the vibrational peak velocity. A statistical analysis is then used to show that this observation, although previously unremarked upon, can be discerned in already published data obtained by others' different techniques.

### II. EXPERIMENTAL DETAILS

The experimental apparatus is illustrated in Fig. 1. The granular material was held in a thin rectangular column with smooth Plexiglas walls, fixed so that only vertical motion was possible. The column inner cross section was  $15 \times 200$  mm, and its height was 500 mm. The column was filled with transparent spherical glass particles of diameter  $d = 0.95 \pm 0.05$  mm to a mean granular bed height,  $h = 75$  mm. The bed, including the container, was subject to vertical vibrational forcing provided by an air-cooled electromagnetically driven shaker (V721, LDS Ltd., Hertfordshire, UK). The vibrational forcing was controlled by a Dactron COMET USB controller (LDS Ltd.) with feedback from two integrated-circuit piezoelectric accelerometers (model 353B03, PCB Piezotronics, Inc., NY, USA) attached to the base of the column. The acceleration and frequency were controlled to a resolution of  $0.005g$  and  $0.01$  Hz, respectively, where  $g$  is the acceleration due to gravity.

The dynamics of the particles in the vibrated bed were studied using DWS in transmission mode [21]. This method involves illuminating one side of the bed at the point of interest with a  $\sim 2$ -mm-diam laser beam and collecting the scattered light from the opposite side of the bed over a time,  $t$ , with a single mode optical fiber (OZ Optics Ltd., Ottawa, Canada). A 400-mW diode-pumped solid-state linearly polarized laser (Torus 532, Laser Quantum Ltd., Cheshire, UK), operating at a wavelength of  $\lambda = 532$  nm in single longitudinal mode, was used. The collected light signal was bifurcated and fed into two matched photomultiplier tubes (PMTs) to reduce spurious correlations due to possible afterpulsing effects of the detector. The outputs from the PMTs were amplified and fed to a multitaup digital correlator (Flex 05, Correlator.com, USA), which performed a pseudo cross-correlation analysis in real time to give the intensity autocorrelation function (IACF),

\*vladimir.zivkovic@adelaide.edu.au

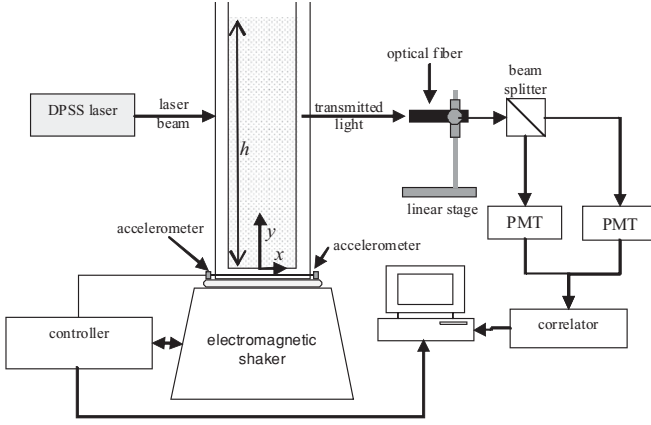


FIG. 1. Schematic of the experimental setup.

$g_2(t)$ , that was stored on a PC for further offline analysis as detailed below.

The vibrated bed was subject to sinusoidal vibrations in all cases reported here. The vertical position of the bed, at time  $t$ , for such vibrational motion is expressed by

$$y_p = A \sin(\omega t), \quad (1)$$

where  $A$  and  $f = \omega/2\pi$  are the amplitude and frequency, respectively. The associated peak vibrational velocity and acceleration of the bed are  $v_p = \omega A$  and  $a_p = \omega^2 A$ , respectively; the latter is expressed here in the nondimensional form,  $\Gamma = a_p/g$ , where  $g$  is the acceleration due to gravity. Note that frequency, amplitude, velocity, and acceleration are related. Knowing any two quantities, the other two can be easily calculated.

The IACF was determined at the centerline of the bed,  $x = 0$  mm, and at vertical position,  $y = 40$  mm, above the base of the bed, which is approximately the center of the bed. The measurements were done at only one position, as our previous experiments found that the granular temperature varied very little with spatial position in the bed [20]. Measurements near the wall, and the top and bottom of the bed where variations may be expected were impossible due to experimental constraints [20,22]. Before each measurement the system was vibrated for at least 10 min, allowing the bed to reach a stationary state. The IACFs were obtained by collecting and correlating ten blocks of data 30 s long each.

The normalized electric-field autocorrelation function (FACF),  $g_1(t)$ , was obtained from the IACF,  $g_2(t)$ , using the Siegert relationship [21,23],

$$g_2(t) \equiv \frac{\langle I(0)\langle I(t) \rangle \rangle}{\langle I \rangle^2} = 1 + \beta |g_1(t)|^2, \quad (2)$$

where  $I$  is light intensity and  $\beta$  is a phenomenological parameter determined from the intercept of the IACF; this phenomenological parameter was always found to be  $\beta \approx 0.5$ , as expected for depolarized light [21].

The mean-square displacement (MSD) of the particles,  $\langle \Delta r^2(t) \rangle$ , was determined by inverting the FACF using the formula [21]

$$g_1(t) = \frac{L/l^* + 4/3}{z_0/l^* + 2/3} \left[ \sinh\left(\frac{z_0}{l^*} \sqrt{X}\right) + \frac{2}{3} \sqrt{X} \cosh\left(\frac{z_0}{l^*} \sqrt{X}\right) \right] \left[ \left(1 + \frac{4}{3} X\right) \sinh\left(\frac{L}{l^*} \sqrt{X}\right) + \frac{4}{3} \sqrt{X} \cosh\left(\frac{L}{l^*} \sqrt{X}\right) \right], \quad (3)$$

where  $X = \langle \Delta r^2 \rangle k^2 + 3l^*/l_a$ ,  $L$  is the sample thickness (15 mm here),  $l^*$  the transport mean free path,  $l_a$  the absorption path length,  $z_0 = \gamma l^*$  the distance over which the incident light is randomized, and  $k = 2\pi/\lambda$  the light wave vector. The scaling factor,  $\gamma$ , was set to unity, in line with common practice [21,24].

The mean square of particle velocity fluctuations about the mean flow velocity can be derived straightforwardly from the ballistic region of the MSD [25], provided it is resolved, using the expression

$$\langle \Delta r^2 \rangle = \langle \delta v^2 \rangle t^2. \quad (4)$$

The granular temperature for a monodisperse granular material flowing in 3D can then be evaluated following [26]:

$$\theta = \frac{1}{3} \langle \delta v^2 \rangle. \quad (5)$$

Equation (3) requires knowledge of the transport mean free path,  $l^*$ , or step size in the random walk of photons, and the diffusive absorption path length,  $l_a$ , which accounts for light absorption, at the positions and conditions considered. In our previous study [20], we used the method of static transmission [21,27] to determine that  $l_a = 4$  mm and that  $l^*$  varies from 1.95 to 2 mm for the amplitude range investigated here of 0.05–0.17 mm.

### III. RESULTS AND DISCUSSION

Figure 2 shows a typical IACF,  $g_2(t)$ , along with the FACF,  $g_1(t)$ , and MSD,  $\langle \Delta r^2(t) \rangle$ , obtained from the analysis outlined in the previous section. The example IACF, shown in Fig. 2(a), first decays from  $g_2 \approx 1.5$  over the time scale of  $10^{-6} - 10^{-5}$  s to an intermediate plateau, where it remains before once again decaying over the time scale of  $10^{-1} - 10^0$  s, this time toward unity. The intercepts of  $g_2$  for all considered vibrational conditions were close to 1.5, the expected value for depolarized light [21]. This value indicates that we are imaging one coherence area and that enough decorrelation cycles have been taken to ensure good statistics.

Figure 2(b) shows that the double decay and time scales seen in the IACF are reflected and enhanced in the FACF, as one would expect given the Siegert relationship, (2). Rigorous interpretation of the long-time behavior is difficult due to limitations of the technique [28]. However, previous work by the authors [20] suggests that it is reasonable to attribute the intermediate plateau and second decay in the ACFs of Fig. 2 to caged motion of particles at intermediate times and, at longer times, particles breaking free of their cages only to become trapped once again in new cages nearby. The MSD obtained from inversion of (3) using the FACF is shown in Fig. 2(c). A quantitative analysis of the ballistic region of this MSD using (4) gives a particle velocity fluctuation  $\langle \delta v^2 \rangle^{1/2} = 2.86$  mm/s. The intermediate plateau in MSD cannot be used

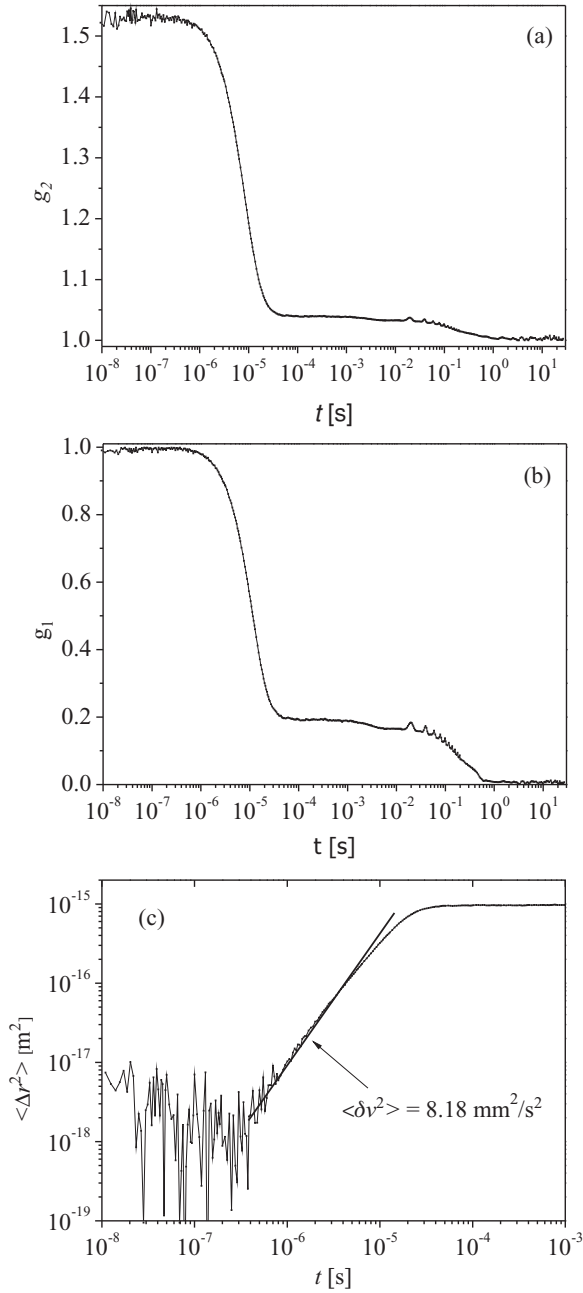


FIG. 2. (a) The intensity autocorrelation function,  $g_2(t)$ , at  $\Gamma = 2.6$  and  $v_p = 40$  mm/s. (b) The normalized electric-field autocorrelation function,  $g_1(t)$ , obtained from  $g_2(t)$  using the Siegert relationship. (c) The MSD obtained from  $g_1(t)$  by inverting (3); the mean square of fluctuating velocity  $\langle \delta v^2 \rangle$  is indicated. The solid line is fitted to (4).

for quantitative analysis due to the limitations of the technique, which is the reason we do not show MSD for times longer than 1 ms [28].

### A. Two-dimensional mapping of granular temperature

Most experimental studies of the granular temperature scaling in a vibrated granular bed are carried out at a fixed frequency [9,11,16,17,19]. Figure 3(a) illustrates that, under this commonly adopted experimental protocol, the

granular temperature is a linear function of the square of peak vibrational velocity, in line with the theoretical prediction [9,10]. However, a linear trend is also obvious when the granular temperature data is replotted against the square of acceleration, Fig. 3(b). This is a straightforward consequence of the fact that acceleration is a linear function of peak velocity at a fixed frequency (viz.,  $\Gamma = \omega v_p$ ). The data shows as well a linear trend with the square of the amplitude (not shown here), because at a fixed vibrational parameter, the other two vibrational parameters are a simple function of peak velocity and that parameter (viz.,  $A = v_p/\omega$ ). This discussion indicates that varying the vibrational peak velocity while fixing the frequency as is commonly practiced does not allow the dependency of the granular temperature on any of the other vibrational parameters to be elucidated.

If we are to determine if the granular temperature is dependent on vibrational parameters beyond the peak velocity, for sinusoidal forcing we must systematically vary two of the vibrational parameters. Based on the widely held view that the granular temperature scales with the square of peak velocity [9–20], it is reasonable to suppose that it should be one of the two parameters. Choice of the second parameter from among the three available (viz., acceleration, amplitude, and frequency) is less obvious. However, we initially selected here the acceleration because (1) its intuitive link to (vibrational) forcing, (2) our previous study of a submerged vibrated bed indicates the granular temperature scales with the acceleration [28], and (3) because its meaning is clearer in other vibrational modes such as, for example, random vibrational forcing [29,30], where amplitude and frequency are less well defined. On this basis, we systematically varied acceleration while keeping the peak velocity fixed and vice versa (i.e., varied the peak velocity while keeping the acceleration fixed) so as to decompose the influence of these two parameters on the granular temperature. Figure 4(a) shows that the granular temperature data obtained in this way is linearly dependent on the square of the peak velocity as expected. However, Fig. 4(b) shows that the granular temperature for a given peak vibrational velocity,  $v_p$ , is not constant at all but, rather, is also linearly correlated with the vibrational acceleration,  $\Gamma$ . Although not previously commented on, as we will show below, careful consideration of the data from previous studies also supports this notion that granular temperature depends on other vibrational parameters, in addition to the square of the peak velocity.

Given this, we plot the granular temperature as a function of both peak velocity and acceleration in Fig. 5. Figure 5 shows (to our knowledge) the first ever map of the granular temperature as a function of the square of peak vibrational velocity and the acceleration. The data is fitted with a multiple linear regression model with two explanatory variables of the following general form (see the Appendix)

$$\theta = b_0 + b_1 v_p^2 + b_2 \Gamma. \quad (6)$$

The overall multiple regression is statistically significant ( $F(2,51) = 870.8$ ,  $p$  value  $\ll 0.001$ , see the Appendix for an explanation of these and other statistical measures used here), and the two variables accounted for  $\sim 97\%$  of the variance

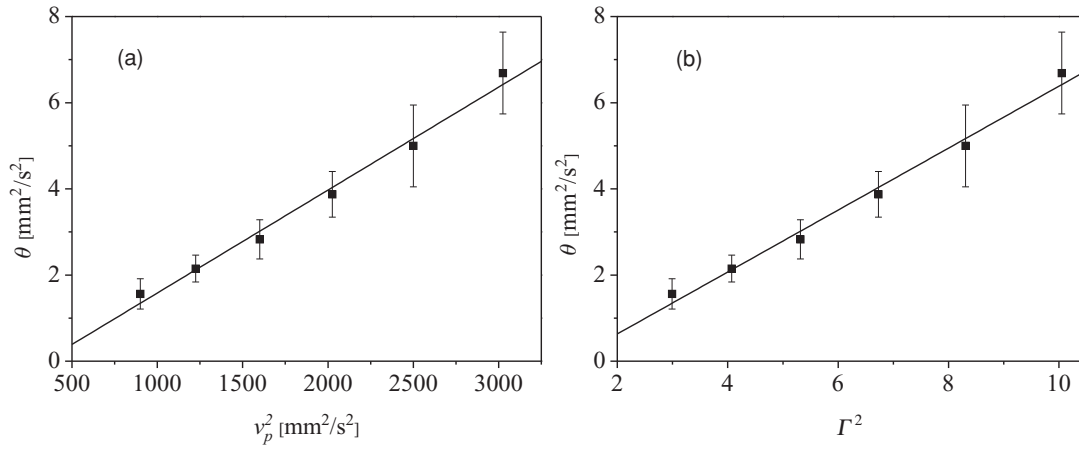


FIG. 3. Variation of the granular temperature,  $\theta$ , for fixed frequency  $f = 90$  Hz with (a) square of peak forcing velocity,  $v_p^2$ , and (b) square of dimensionless accelerations,  $\Gamma^2$ . Error bars are standard deviations of the ten correlation measurements and lines are a linear fit to the data.

in the granular temperature data (i.e., the coefficient of determination  $R^2 = 0.9715$ , adjusted  $R^2 = 0.9705$ ). A comparison with the coefficient of determination for the univariate scaling involving the square of the peak velocity only (Table I) clearly indicates that the commonly held belief that the granular temperature varies only with the peak velocity is questionable. The multiple linear regression model also has a smaller prediction error sum of squares (PRESS) value (Table I), which is further proof that addition of the acceleration term to the scaling model is justified. More importantly, as also shown in Table I, the greater-than-10 difference in the Bayesian information criterion (BIC) represents conclusive evidence of the relative superiority of a bivariate over the univariate scaling model (see the Appendix for an explanation of PRESS and BIC).

Further support for the assertion that the bivariate scaling of (6) is superior to the univariate scaling is provided by the  $t$  and  $p$  values for the bivariate scaling coefficients (Table II), which show that both of the explanatory variables are statistically significant (see the Appendix for an explanation of the  $t$  and

$p$  values). The values of the standardized coefficients for the square of the peak velocity,  $\beta_1$ , and the dimensionless acceleration,  $b_2$ , which are also shown in Table II, indicate that while the square of the peak velocity is the leading scaling parameter, the acceleration also has a substantial effect on the granular temperature (see the Appendix for an explanation of the standardized coefficients).

While the analysis above indicates the bivariate scaling of (6) is superior to the commonly used univariate scaling, it is necessary to test if the acceleration is the most appropriate second scaling parameter. The BIC values in Table I indicate that the amplitude is unlikely to be the most appropriate second scaling parameter. The small difference between the BIC values of the frequency- and acceleration-based scalings means, on the other hand, that either acceleration or frequency may be an appropriate second scaling parameter (see the Appendix for an explanation of differences in the BIC). Use of acceleration as the second scaling parameter as done here is, therefore, not unreasonable given the advantages it brings, as outlined above.

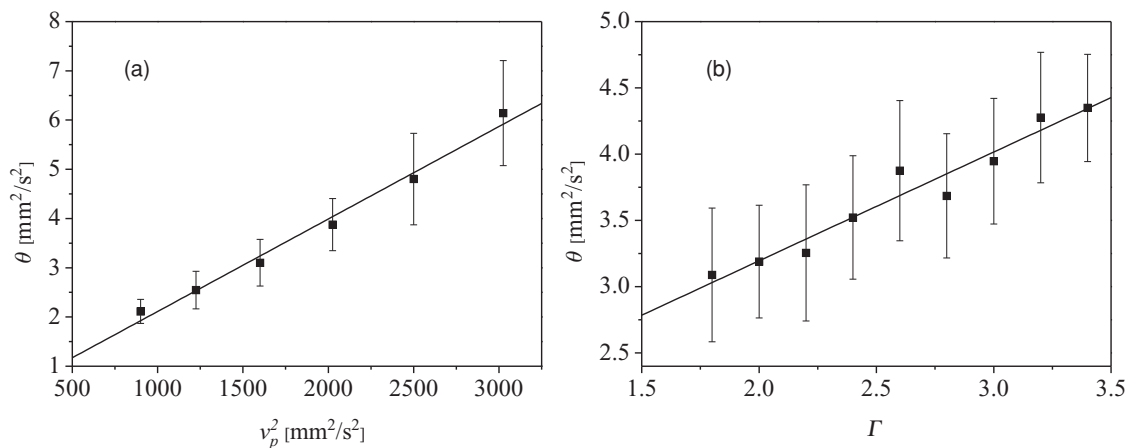


FIG. 4. Variation of the granular temperature,  $\theta$ , with (a) square of peak vibrational velocity at fixed dimensionless acceleration  $\Gamma = 2.6$ , and (b) acceleration at fixed peak vibrational velocity  $v_p = 45$  mm/s. Error bars are standard deviations of the ten correlation measurements and lines are a linear fit to the data.

TABLE I. Model selection criteria for the common univariate and the various possible bivariate granular temperature (GT) scaling models involving the peak vibrational velocity.

Model variables	$R^2$	Adjusted $R^2$	PRESS	BIC	VIF
$v_p^2$	0.8135	0.8099	19.70	160.3	
$v_p^2$ and $\Gamma$	0.9715	0.9704	3.14	62.8	1.00
$v_p^2$ and $f$	0.9725	0.9714	3.09	60.9	1.94
$v_p^2$ and $A$	0.9578	0.9562	4.72	84.0	4.00

### B. Reexamination of previously published data

In order to check the observations arising from our DWS data obtained in the study reported above, we performed the same detailed regression analysis of previously published experimental data [12,14,20]. The results of this analysis are shown in Tables III and IV.

Table III shows that, except for the  $v_p^2-f$  regression model of the Zivkovic *et al.* [20] data, all the multiple regression models with two variables have larger  $R^2$  and smaller PRESS values as compared to the univariate model. Furthermore, differences in BIC are  $\sim 6$  or more (except for above-mentioned case), which represents strong evidence in favor of the bivariate models. This provides further proof that granular temperature scales with two vibrational parameters rather than just the square of the peak velocity. Although for all three previous studies the selection criteria suggests that amplitude is the “best” choice for the second scaling parameter, collinearity between the square of the peak velocity and amplitude is a serious issue for two of them [12,20], as indicated by the variance inflation factor (VIF) being greater than 5 (Table III—see the Appendix for an explanation of the VIF). In the case of the Losert *et al.* [14] data, the

small sample size means conclusions drawn from this study cannot be considered to be particularly reliable (the common recommendation is seven to ten experimental or observational point for *each* explanatory variable in the model [31]). In contrast, the bivariate model with amplitude is considerably worse for the study reported here, as shown in Table III. Finally, bivariate models with acceleration and frequency are essentially indistinguishable from each other as the differences in the BIC between these models for all studies are very small ( $\sim 2$ ). These less-than-conclusive and, in places, contradictory findings make it difficult to be definitive about which of the frequency or acceleration should be used with the square of the peak vibrational velocity to best correlate the granular temperature in vibrated granular systems. Future experimental and theoretical considerations are needed to elucidate this further.

Although the above analysis does not provide unquestionable support for acceleration as the “best” choice for the second scaling parameter, it certainly does not provide a basis for rejection of this hypothesis. Therefore, for comparison, we did a regression analysis of previously published data using the dimensionless acceleration as the second scaling parameter. Table IV shows  $t$ -test results for both the square of the peak velocity and acceleration terms in a multiple linear regression model for the data from this and the three previous experimental studies. As expected, the large  $t$  values and very small  $p$  values indicate that the square of peak velocity is a statistically more important parameter in the model. Nonetheless, the acceleration terms are statistically significant at the commonly applied threshold for model coefficients (i.e., 95% confidence level) except for the most dilute case ( $c = 0.28$ ) of the Losert *et al.* [14] data. Furthermore, the acceleration term is even highly significant (i.e., 99.9% confidence) for the Tai *et al.* [12] data. The fact that the standardized coefficient for the square of the peak velocity is several times greater than that of the acceleration coefficients (Table IV) indicates that the former is the leading scaling variable.

The nonstandardized scaling coefficients shown in Table IV for this and our previous study [20] are of the same magnitude. However, the frequency scaling coefficients are of opposite sign. This contradiction may arise from the main difference between the two systems, the excitation mechanism: while in this study we vibrated the whole box as in the other two studies [12,14] in our previous study a vibrating piston supplied energy to the granular system [20]. The scaling coefficients for the other two studies [12,14], are orders of magnitude greater than the ones presented here and different between each other. Once again, this difference arises from the different experimental apparatus and conditions—one is for a highly fluidized shallow dilute 3D bed [14] and the other is a similarly fluidized 2D system [12].

### IV. CONCLUSION

Diffusing wave spectroscopy, which is a highly sensitive yet versatile method relative to other previously exploited methods, has been used to measure the granular temperature of 0.95 mm glass particles in a dense three-dimensional vibrated granular bed under sinusoidal driving. Although a

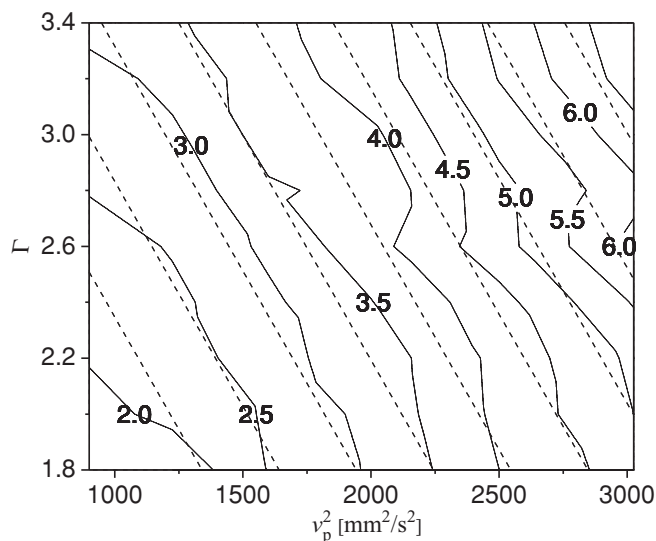


FIG. 5. Contour plot of the granular temperature,  $\theta$  in  $\text{mm}^2/\text{s}^2$ , in the vibrated bed as a function of the square of peak vibrational velocity,  $v_p^2$ , and the dimensionless acceleration,  $\Gamma$ . Solid lines are experimental granular isotherms; dashed lines are a multiple linear regression model fitting, (6).

TABLE II. Summary of coefficient for bivariate linear regression fitting, (6).

Variable	Unstandardized coefficient, $b$	Standard error	Standardized coefficient, $\beta$	$t$ for $H_0$ coefficient = 0	$p$ value
Constant	-2.081	0.182			
$v_p^2$	0.0016	0.00004	0.902	38.19	$3.45 \times 10^{-39}$
$\Gamma$	1.032	0.0613	0.398	16.83	$1.81 \times 10^{-22}$

statistical analysis of this data confirmed that the square of the peak vibrational velocity is the leading parameter in scaling of granular temperature, in line with theory and previous experiments, a significant correlation was observed with the other vibrational parameters—the frequency, acceleration, and amplitude. A further statistical analysis of the data was undertaken to determine which of these three is the most appropriate second scaling parameter (only two are required to specify the remainder). Although this analysis indicated that the amplitude was not the most appropriate, it could not differentiate between the remaining two. A similar statistical analysis of previously published data was also undertaken here with similar conclusions. Future work is, therefore, required to determine which is the most appropriate second scaling parameter—acceleration or frequency. Consideration should also be given to how the conclusions drawn here are affected

by other details of the vibrational system, such as granular bed height, coefficient of restitution, particle size, driving force mode (e.g., random, square wave), and boundary conditions.

**APPENDIX: MULTIPLE LINEAR REGRESSION ANALYSIS**

Simple linear regression considers a single explanatory or regressor variable  $x$  and a dependent or response variable  $y$  [32,33]. It is assumed that each observation,  $y$ , can be described by the univariate model

$$y = b_0 + b_1x + \varepsilon, \tag{A1}$$

where the intercept  $b_0$  and slope  $b_1$  are unknown regression coefficients, and  $\varepsilon$  is a random error with zero mean. On the other hand, multiple linear regression admits the possibility of more than one explanatory variable. The general form of the

TABLE III. Model selection criteria for common univariate and various bivariate GT scaling models. Variance inflation factor (VIF) is given for a multiple regression models with two variables. The experimental sample size,  $n$ , is specified for each study. Note: For Losert *et al.* [14] the reported  $c$  is coverage, which is principally connected to the solid fraction of the system.

DATA	Model predictors	$R^2$	Adjusted $R^2$	PRESS	BIC	VIF
This study $n = 54$	$v_p^2$	0.8135	0.8099	19.70	160.3	
	$v_p^2$ and $\Gamma$	0.9715	0.9704	3.14	62.8	1.00
	$v_p^2$ and $f$	0.9725	0.9714	3.09	60.9	1.94
	$v_p^2$ and $A$	0.9578	0.9562	4.72	84.0	4.00
Losert <i>et al.</i> [14] (Fig. 6) $n = 9$ ( $c = 0.70$ )	$v_p^2$	0.9895	0.9880	$4.42 \times 10^7$	151.6	
	$v_p^2$ and $\Gamma$	0.9970	0.9960	$2.18 \times 10^7$	142.5	1.12
	$v_p^2$ and $f$	0.9923	0.9897	$3.67 \times 10^7$	151.0	1.86
	$v_p^2$ and $A$	0.9979	0.9973	$1.27 \times 10^7$	139.1	3.29
Losert <i>et al.</i> [14] (Fig. 6) $n = 9$ ( $c = 0.42$ )	$v_p^2$	0.9842	0.9820	$1.70 \times 10^8$	161.3	
	$v_p^2$ and $\Gamma$	0.9923	0.9898	$1.22 \times 10^8$	157.0	1.12
	$v_p^2$ and $f$	0.9906	0.9874	$1.25 \times 10^8$	158.9	1.86
	$v_p^2$ and $A$	0.9989	0.9986	$1.67 \times 10^7$	139.3	3.29
Losert <i>et al.</i> [14] (Fig. 6) $n = 9$ ( $c = 0.28$ )	$v_p^2$	0.9730	0.9691	$3.98 \times 10^8$	168.0	
	$v_p^2$ and $\Gamma$	0.9831	0.9775	$3.34 \times 10^8$	166.0	1.12
	$v_p^2$ and $f$	0.9840	0.9787	$3.12 \times 10^8$	165.5	1.86
	$v_p^2$ and $A$	0.9957	0.9943	$8.76 \times 10^7$	153.6	3.29
Tai and Hsiau [12] [Fig. 8(c)] $n = 19$	$v_p^2$	0.9051	0.8995	$1.38 \times 10^4$	180.5	
	$v_p^2$ and $\Gamma$	0.9550	0.9493	$8.02 \times 10^3$	169.2	2.07
	$v_p^2$ and $f$	0.9515	0.9454	$8.48 \times 10^3$	170.6	1.34
	$v_p^2$ and $A$	0.9699	0.9661	$5.21 \times 10^3$	161.6	7.34
Zivkovic <i>et al.</i> [20] (Fig. 9) $n = 17$	$v_p^2$	0.9628	0.9603	176.76	85.3	
	$v_p^2$ and $\Gamma$	0.9765	0.9731	137.75	80.3	1.21
	$v_p^2$ and $f$	0.9673	0.9626	188.16	85.9	1.32
	$v_p^2$ and $A$	0.9889	0.9874	59.15	67.5	9.50

TABLE IV. Summary of coefficient for bivariate linear regression fitting, Eq. (6). The experimental sample size,  $n$ , is specified for each study. Note: For Losert *et al.* [14] the reported  $c$  is coverage, which is principally connected to the solid fraction of the system.

Data	Predictor	Unstandardized coefficient, $b$	Standard error	Standardized coefficient, $\beta$	$t$ for $H_0$ coefficient = 0	$p$ value
This study $n = 54$	Constant	-2.081	0.182			
	$v_p^2$	0.0016	0.00004	0.902	38.19	$3.45 \times 10^{-39}$
	$\Gamma$	1.032	0.0613	0.398	16.83	$1.81 \times 10^{-22}$
Losert <i>et al.</i> [14] (Fig. 6) $n = 9$ ( $c = 0.70$ )	Constant	-2077	716.0			
	$v_p^2$	1.043	0.026	0.964	40.69	$1.47 \times 10^{-8}$
	$\Gamma$	805.1	207.9	0.092	3.87	$8.23 \times 10^{-3}$
Losert <i>et al.</i> [14] (Fig. 6) $n = 9$ ( $c = 0.42$ )	Constant	-3754	1607			
	$v_p^2$	1.458	0.058	0.960	25.32	$2.50 \times 10^{-7}$
	$\Gamma$	1177	466.6	0.096	2.52	$4.50 \times 10^{-2}$
Losert <i>et al.</i> [14] (Fig. 6) $n = 9$ ( $c = 0.28$ )	Constant	-4659	2647			
	$v_p^2$	1.600	0.095	0.951	16.88	$2.76 \times 10^{-6}$
	$\Gamma$	1457	768.5	0.107	1.90	$1.07 \times 10^{-1}$
Tai and Hsiau [12] [Fig. 8(c)] $n = 19$	Constant	-23.23	13.46			
	$v_p^2$	0.055	0.006	0.720	9.42	$6.22 \times 10^{-8}$
	$\Gamma$	18.64	4.429	0.322	4.21	$6.65 \times 10^{-4}$
Zivkovic <i>et al.</i> [20] (Fig. 9) $n = 17$	Constant	2.815	1.817			
	$v_p^2$	0.0035	0.00016	1.035	22.96	$1.64 \times 10^{-12}$
	$\Gamma$	-1.818	0.6355	-0.129	-2.86	$1.26 \times 10^{-2}$

multiple regression model with  $k$  regressor variables is

$$y = b_0 + b_1x_1 + b_2x_2 + \dots + b_kx_k + \varepsilon, \quad (\text{A2})$$

where  $b_0, b_1, b_2, \dots, b_k$  are the regression coefficients. This model describes a hyperplane in the  $k$ -dimensional space of the regressor variables  $x_0, x_1, x_2, \dots, x_k$ .

The test for significance of regression, which can be calculated from the analysis of variance for the regression, has an  $F$  distribution with  $k$  and  $n-(k-1)$  degrees of freedom, where  $n$  is the sample size. The null hypothesis that all the coefficients are zero can be rejected if an  $F$  value is large, i.e., the corresponding  $p$  value is very close to zero [32,33]. The null hypothesis for testing the significance of any *individual* regression coefficient has a  $t$  distribution with  $n-(k-1)$  degrees of freedom [32,33]. Basically, the larger the value of  $t$  and smaller the corresponding  $p$  value, the greater is the contribution of that variable to the model. A commonly applied threshold for rejection of a model coefficient is at the probability level of  $p = 0.05$  (i.e., 95% confidence level) [32,33].

The coefficient of determination  $R^2$  is a measurement of regression fit, and it represents the proportion of total variation in a dependent variable explained by the regression model [32,33]. Because  $R^2$  can only increase, and never decline, when explanatory variables are added, a ‘‘penalized’’ value of  $R^2$  by a correction for degrees of freedom, the adjusted  $R^2$  that does not necessarily increase with model complexity, is used for model comparison.

Another simple criterion for model comparison is PRESS. A small PRESS value is associated with a good model in the sense that it yields small prediction errors [32]. A more sophisticated measure that penalizes model complexity is the BIC [33]. Models with smaller BIC values are better. Moreover, the difference between the BIC values of different models can be interpreted as follows: according to Raftery [34], a difference in BIC of less than 2 provides weak evidence, a difference between 2 and 6 positive evidence, between 6 and 10 strong evidence, and greater than 10 very strong evidence for the relative superiority of one model over the other.

Different regressor variables in a regression analysis generally have different metrics. The standardized coefficients  $\beta$ 's place all variables on the same metrics (standard deviation units), enabling a limited comparison of the relative impact of incommensurable variables in a regression equation for the same sample [33]. However,  $\beta$ 's cannot be used to compare effects across different studies and samples, where nonstandardized coefficient  $b$ 's have to be used.

When undertaking a multiple linear regression analysis, care must be exercised to avoid issues such as collinearity and variance inflation. Multicollinearity, or dependence between explanatory variables, can result in misleading regression results [32,33]. The VIF is the basic diagnostic for multicollinearity, with VIF larger values indicating its presence [32,33]. The common rule of thumb is 10 [32,33], but other authors consider this value too liberal and suggest that VIF should not exceed 4 or 5 [32].

- [1] S. Ogawa, in *Proceedings of the US-Japan Seminar on Continuum Mechanical and Statistical Approaches in the Mechanics of Granular Materials*, edited by S. C. Cowin and M. Satake (Gakajutsu Bunken Fukyu-Kai, Tokyo, 1978), pp. 208–217.
- [2] J. T. Jenkins and S. B. Savage, *J. Fluid. Mech.* **130**, 187 (1983).
- [3] C. K. K. Lun *et al.*, *J. Fluid. Mech.* **140**, 223 (1984).
- [4] M. L. Hunt, *Int. J. Heat Mass Transfer* **40**, 3059 (1997).
- [5] L. Huilin, H. Yurong, and D. Gidaspow, *Chem. Eng. Sci.* **58**, 1197 (2003).
- [6] R. W. Lyczkowski and J. X. Bouillard, *Prog. Energy Combust. Sci.* **28**, 543 (2002).
- [7] C. S. Campbell, *Acta Mech.* **104**, 65 (1994).
- [8] H. S. Tan, A. D. Salman, and M. J. Hounslow, *Chem. Eng. Sci.* **61**, 3930 (2006).
- [9] S. Warr, J. M. Huntley, and G. T. H. Jacques, *Phys. Rev. E* **52**, 5583 (1995).
- [10] V. Kumaran, *Phys. Rev. E* **57**, 5660 (1998).
- [11] K. Feitosa and N. Menon, *Phys. Rev. Lett.* **88**, 198301 (2002).
- [12] C. H. Tai and S. S. Hsiau, *Powder Technol.* **139**, 221 (2004).
- [13] E. Falcon *et al.*, *Europhys. Lett.* **74**, 830 (2006).
- [14] W. Losert *et al.*, *Chaos* **9**, 682 (1999).
- [15] H.-Q. Wang, K. Feitosa, and N. Menon, *Phys. Rev. E* **80**, 060304 (2009).
- [16] R. D. Wildman and J. M. Huntley, *Phys. Fluids* **15**, 3090 (2003).
- [17] R. D. Wildman, J. M. Huntley, and D. J. Parker, *Phys. Rev. E* **63**, 061311 (2001).
- [18] S. Luding, H. J. Herrmann, and A. Blumen, *Phys. Rev. E* **50**, 3100 (1994).
- [19] S. Y. You and H. K. Pak, *J. Korean Phys. Soc.* **38**, 577 (2001).
- [20] V. Zivkovic *et al.*, *Powder Technol.* **182**, 192 (2008).
- [21] D. A. Weitz and D. J. Pine, in *Dynamic Light Scattering: The Method and Some Applications*, edited by W. Brown (Clarendon, Oxford, UK, 1993), pp. 652–720.
- [22] V. Zivkovic *et al.*, *Chem. Eng. Sci.* **64**, 1102 (2009).
- [23] J. B. Berne and R. Pecora, *Dynamic Light Scattering* (Wiley-Interscience, New York, 1976).
- [24] L. Xie *et al.*, *Europhys. Lett.* **74**, 268 (2006).
- [25] N. Menon and D. J. Durian, *Science* **275**, 1920 (1997).
- [26] M. J. Biggs and D. H. Glass, *Powder Technol.* **182**, 127 (2008).
- [27] W. Leutz and J. Rička, *Opt. Commun.* **126**, 260 (1996).
- [28] V. Zivkovic, M. J. Biggs, and D. H. Glass, *J. Phys. D* **42**, 245404 (2009).
- [29] P. Mayor *et al.*, *New J. Phys.* **7**, 28 (2005).
- [30] G. D’Anna *et al.*, *Nature (London)* **424**, 909 (2003).
- [31] M. Kutner *et al.*, *Applied Linear Statistical Models* (McGraw-Hill/Irwin, New York, 2004).
- [32] D. C. Montgomery and G. C. Runger, *Applied Statistics and Probability for Engineers*, 3rd ed. (Wiley, New York, 2003).
- [33] J. Fox, *Applied Regression Analysis and Generalized Linear Models* (Sage, Los Angeles, CA, 2008), p. 665.
- [34] A. E. Raftery, *Sociological Methodology* **25**, 111 (1995).